

# The Effect of Replacement of Zn<sup>2+</sup> Cation with Ni<sup>2+</sup> Cation on the Structural Properties of Ba<sub>2</sub>Zn<sub>1-x</sub>Ni<sub>x</sub>WO<sub>6</sub> Double Perovskite Oxides (X = 0, 0.25, 0.50, 0.75, 1)

Yousif A. Alsabah<sup>1,2</sup>, Abdelrahman A. Elbadawi<sup>1</sup>, Eltayeb M. Mustafa<sup>1</sup>, Mohamed A. Siddig<sup>1,3</sup>

<sup>1</sup>Department of Physics, Faculty of Science and Technology, Al Neelain University, Khartoum, Sudan

<sup>2</sup>Department of Physics, Faculty of Education and Applied Science, Hajjah University, Hajjah, Yemen

<sup>3</sup>Department of Physics, Faculty of Science, Al Baha University, Al Baha, Saudi Arabia

Email: y.a.alsabah@gmail.com

Received 5 January 2016; accepted 12 February 2016; published 17 February 2016

Copyright © 2016 by authors and Scientific Research Publishing Inc.

This work is licensed under the Creative Commons Attribution International License (CC BY).

<http://creativecommons.org/licenses/by/4.0/>



Open Access

---

## Abstract

The Ba<sub>2</sub>Zn<sub>1-x</sub>Ni<sub>x</sub>WO<sub>6</sub> double perovskite oxides were synthesized using solid state reaction method. The effect of replacement of Zn<sup>2+</sup> with Ni<sup>2+</sup> cation on the structural properties was investigated by X-ray diffraction (XRD) at room temperature. From the X-ray diffraction and by means of standard Rietveld method, the samples showed the same cubic crystal structure with (Fm-3m) space group and the crystallite size ranging from 71.91 nm to 148.71 nm. The unit cell volume was found to decrease as a result of the replacement, while there was no significant difference in the value of tolerance factor of the samples. This is may be due to the convergence of ionic radii of Ni<sup>2+</sup> and Zn<sup>2+</sup> cations. The Fourier Transform Infrared Spectroscopy (FTIR) was performed for the samples and the resultant characteristic absorption bands confirmed the double perovskite structure.

## Keywords

Double Perovskite, XRD, FTIR, Solid State Reaction Method, Tolerance Factor

---

## 1. Introduction

Many authors were interested in the study and preparation of the new double perovskite materials. The general chemical formula of double perovskite oxides was expressed as A<sub>2</sub>BB'O<sub>6</sub>, where A is occupied by an element of group one or group two such as Ca, Sr or Ba and B, B' site is occupied by a translational element, while the O

**How to cite this paper:** Alsabah, Y.A., Elbadawi, A.A., Mustafa, E.M. and Siddig, M.A. (2016) The Effect of Replacement of Zn<sup>2+</sup> Cation with Ni<sup>2+</sup> Cation on the Structural Properties of Ba<sub>2</sub>Zn<sub>1-x</sub>Ni<sub>x</sub>WO<sub>6</sub> Double Perovskite Oxides (X = 0, 0.25, 0.50, 0.75, 1). *Journal of Materials Science and Chemical Engineering*, 4, 61-70. <http://dx.doi.org/10.4236/msce.2016.42007>

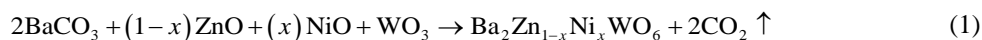
atom is located in between, forming the alternate  $\text{BO}_6$  octahedral and B-O-B bonds. The wide variety of double perovskite materials is due to the alternation of the magnetic and non-magnetic B and B' elements [1] [2]. In particular, the compositions  $\text{A}_2\text{BMoO}_6$ , where B = Fe, Mn or Cr are magnetic ions, are currently studied for their potentiality as magnetoresistive and thermoelectric systems [3].

Synthesize of  $\text{Sr}_2\text{CaW}_x\text{Mo}_{1-x}\text{O}_6$  double perovskite series by solid state reaction was carried out by Zhou *et al.* [4]. The self-activated host material emits strong blue lights at round 435 nm and 468 nm, while the excitation emits at or near UV at about 290 nm due to W-O charge transfer transition. Tian *et al.* [5] studied the crystal structure and magnetic properties of  $\text{Sr}_2\text{MWO}_6$  (M = Co or Ni), using sol-gel method, showing tetragonal (I4/m) structure and homogeneous grain size. The magnetic parameters of the material refer to paramagnetic behavior. The magnetic momentum originates mainly from the interaction between the  $\text{Ni}^{2+}$  ions and  $\text{Co}^{2+}$  ions in  $\text{Sr}_2\text{NiWO}_6$ ,  $\text{Sr}_2\text{CoWO}_6$  respectively. Manoun *et al.* [6] investigated the effect of temperature in the structure of  $\text{Sr}_2\text{ZnWO}_6$  and  $\text{Sr}_2\text{CoWO}_6$  double perovskite oxides when characterized by Raman spectroscopy. The first phase transition from monoclinic (P21/n) crystal structure to tetragonal (I4/m) crystal structure occurred at  $80^\circ\text{C}$ , while the second transition to cubic (Fm-3m) occurred at  $480^\circ\text{C}$ . The effect of the preparation methods on the catalytic activity of the  $\text{LaSrFeMo}_{0.9}\text{Co}_{0.1}\text{O}_6$  methane combustion double perovskite oxide was studied by Zheng *et al.* [7] using two methods; co-precipitation and sol-gel. The sol-gel method had greater impacts on the catalytic activity than co-precipitation method. The  $\text{Ca}_2\text{NiWO}_6$  double perovskite oxide structure and magnetic behavior at  $1150^\circ\text{C}$  with P21/n space group monoclinic crystal structure was investigated by Lopez *et al.* [8].  $\text{Ba}_2\text{MgWO}_6$  and  $\text{Ba}_2\text{ZnWO}_6$  double perovskite oxides were synthesized using the solid state method by Bugaris *et al.* [9]. They characterized the samples by single-crystal X-ray diffraction, Neutron diffraction, UV-visible spectrometry and LS 55 Fluorescence Spectrometer. The cubic (Fm-3m) crystal structure was obtained.

In this work, the  $\text{Ba}_2\text{Zn}_{x-1}\text{Ni}_x\text{WO}_6$  double perovskite oxides were synthesized using solid state reaction method. The aim was to investigate the effect of replacement of  $\text{Zn}^{2+}$  cation with  $\text{Ni}^{2+}$  cation. The X-ray diffraction (XRD) and Fourier Transform Infrared Spectroscopy (FTIR) were used in order to explore the effect of replacement on the structural properties of  $\text{Ba}_2\text{Zn}_{x-1}\text{Ni}_x\text{WO}_6$  double perovskite oxides.

## 2. Experimental

The new samples of double perovskite oxides were synthesized using solid state interaction method and many different treatments were applied in order to get single phase for the samples. The samples were prepared by mixing stoichiometric amounts of ZnO, NiO,  $\text{WO}_3$  and  $\text{BaCO}_3$  and these chemicals were purchased from Alfa Acer of purity 99.9% in order to prepare the  $\text{Ba}_2\text{Zn}_{1-x}\text{Ni}_x\text{WO}_6$  double perovskite oxides. The mixtures of compounds grinded in agate mortar with the addition of acetone and then kept in crucibles and heated in air at  $800^\circ\text{C}$  for 12 hours. The samples pellet in around shape and heated in at  $1000^\circ\text{C}$  and  $1200^\circ\text{C}$ , respectively. Every step of heating treatment was repeated twice with the rate of  $10^\circ\text{C}$  per minute during the heating process and cooling as well. The compound permeated every time grinding with the addition of acetone. The ratio of the amounts calculated was by the following equation:



The X-ray diffractometer (Model Bruker D-8) using  $\text{Cu-K}_\alpha$  radiation ( $\lambda = 1.5406 \text{ \AA}$ ) and a nickel filter operating at 40 KV and 40 mA at scanning the samples was used at room temperature. The data were collected for the  $2\theta$  range  $20^\circ - 80^\circ$  at step size of 0.02 and count time of 5 s. The collected data were then fed to full Prof suite [10] for determination of the lattice parameters, space group, atom's positions and crystalline size ( $D$ ) using Scherer equation [11].

$$D = \frac{0.94\lambda}{\beta_{1/2} \cos(\theta)} \quad (2)$$

where  $D$  is crystallite size,  $\lambda$  is the wavelength of X-ray and  $\beta_{1/2}$  is the half full width of the peaks.

The tolerance factor [12] [13] for the samples calculated by

$$t = \frac{(r_A + r_o)}{\sqrt{2} \left( \left( \frac{1-x}{2} \right) r_B + \left( \frac{x}{2} \right) r'_B + \frac{1}{2} r''_B + r_o \right)} \quad (3)$$

A Fourier transform infrared spectroscopy (FTIR) spectrum was recorded in transmittance mode at room temperature using KBr pellet method, the samples were diluted in KBr of ratio 1:100 for FTIR measurement between 400 and 2000  $\text{cm}^{-1}$  the FTIR of samples were carried out with a (Satellite FTIR 5000 of the wavelength range of 400 to 4000  $\text{cm}^{-1}$ ) [14] where the characteristic bands and peaks of perovskite structure can be assigned.

### 3. Results and Discussion

#### 3.1. The XRD Results

The study and determination of the structural properties of perovskite oxide compounds are very important; such as lattice parameter, space group, type of crystal, atomic position, and molecular binding because they predict and expect the electrical, optical and magnetic properties of materials [15]. The X-ray powder diffraction obtained for  $\text{Ba}_2\text{Zn}_{1-x}\text{Ni}_x\text{WO}_6$  where ( $x = 0, 0.25, 0.50, 0.75, 1$ ) double perovskite series prepared by the solid state reaction is shown in **Figure 1**. The difference in lattice parameters for each sample is shown by the different peaks position in **Figure 2**. The shift in reflection positions is referred to the differences in lattice parameters of unit cells of the samples. The peaks appeared at low intensity in the XRD pattern shown in **Figure 1** are attributed to  $(\text{Ba}_2\text{WO}_5/\text{Ba}_2\text{WO}_4)$  impurities following Manoun *et al.* [16].

#### 3.2. XRD Refined Result

The XRD data of each sample of series are refined by Retiveld method. All samples obtained are showed cubic structure with (Fm-3m) space group. **Table 1** shows the atom positions, the space groups and the lattice parameters of the samples. **Figures 3(a)-(e)** show the refined XRD patterns of the  $\text{Ba}_2\text{Zn}_{1-x}\text{Ni}_x\text{WO}_6$  double perovskite series where  $x = 0, 0.25, 0.50, 0.75, 1$ . In the case of **Figure 3(c)**, the XRD refinement of  $\text{Ba}_2\text{Zn}_{0.50}\text{Ni}_{0.50}\text{WO}_6$  is shown, which represents (Fm-3m) cubic structure with  $a = b = c = 8.097554 \text{ \AA}$ ,  $\alpha = \beta = \gamma = 90$  lattice parameters with  $x = 0.50$ . It is clear that the shift is dependent on the ratio of replacement. Bugaris *et al.* [9] found similar results

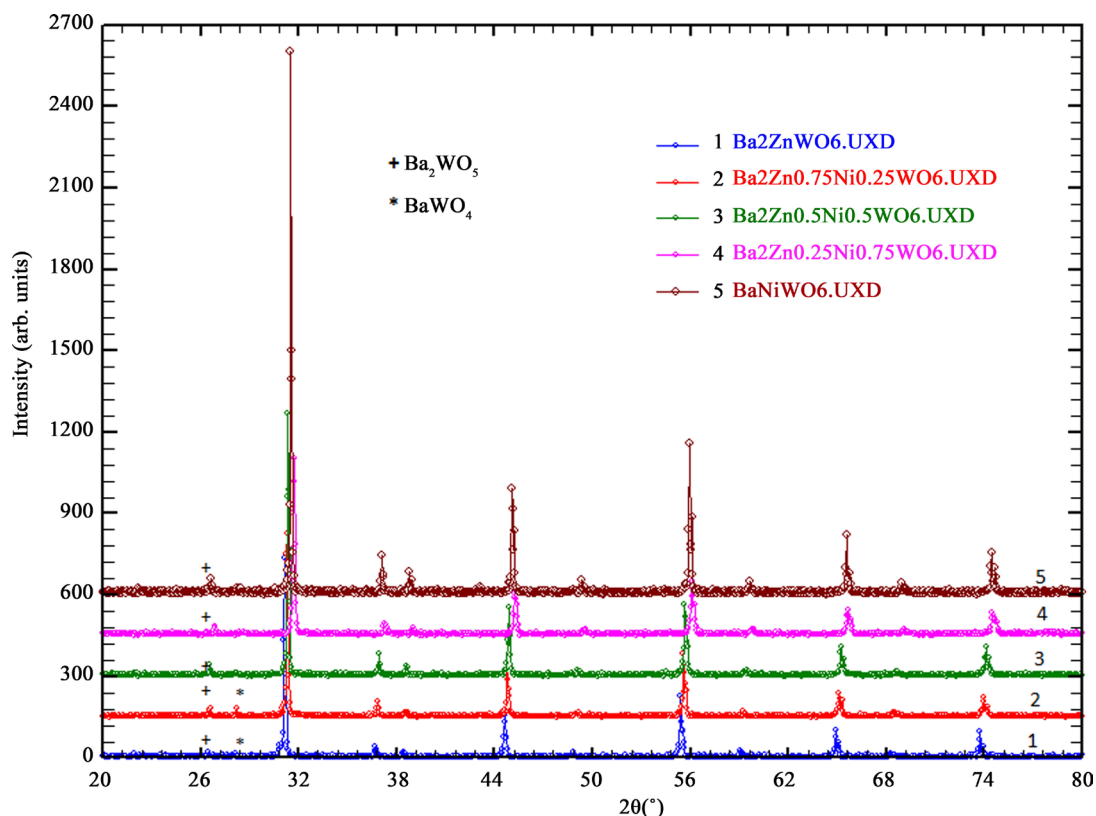


**Figure 1.** X-ray powder diffraction of  $\text{Ba}_2\text{Zn}_{1-x}\text{Ni}_x\text{WO}_6$  double perovskite oxides series.

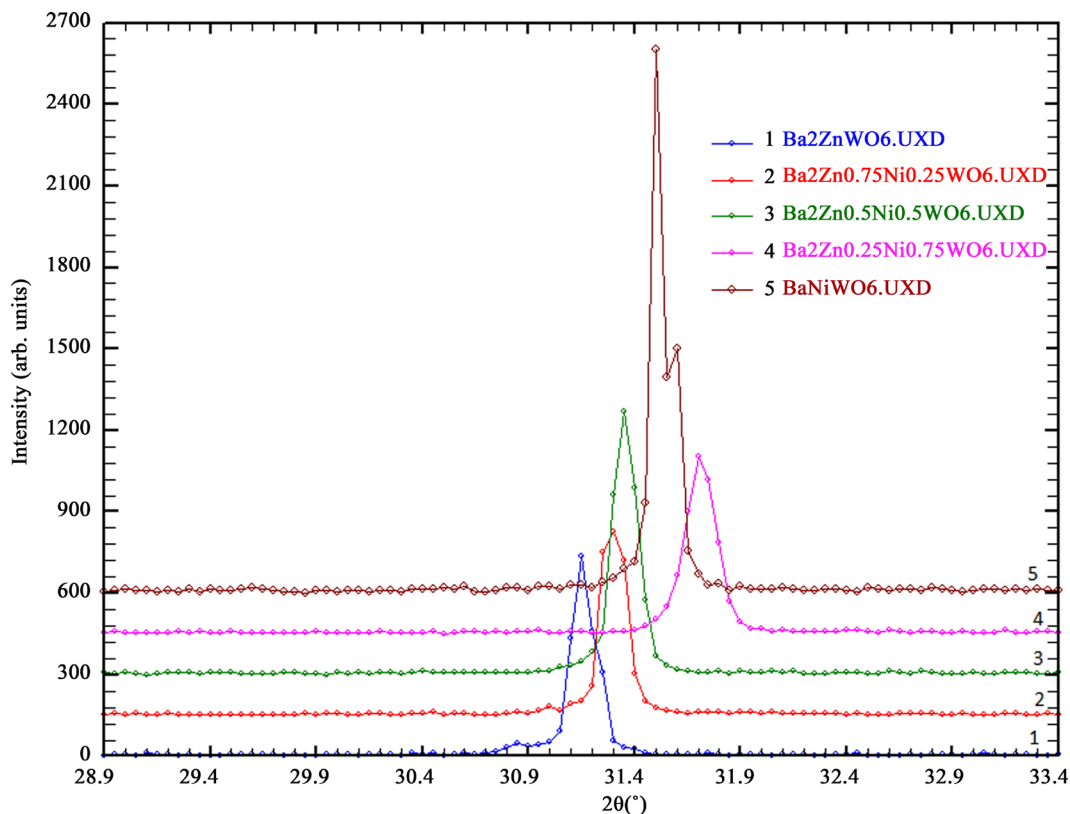
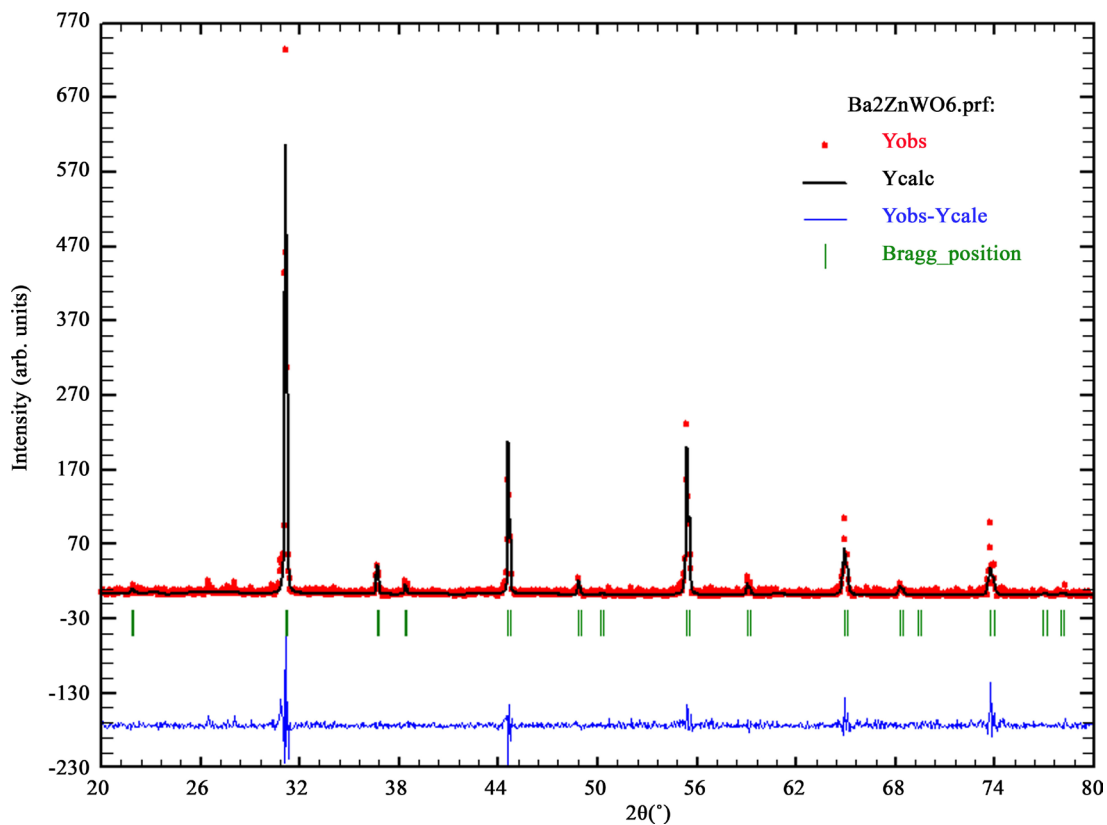


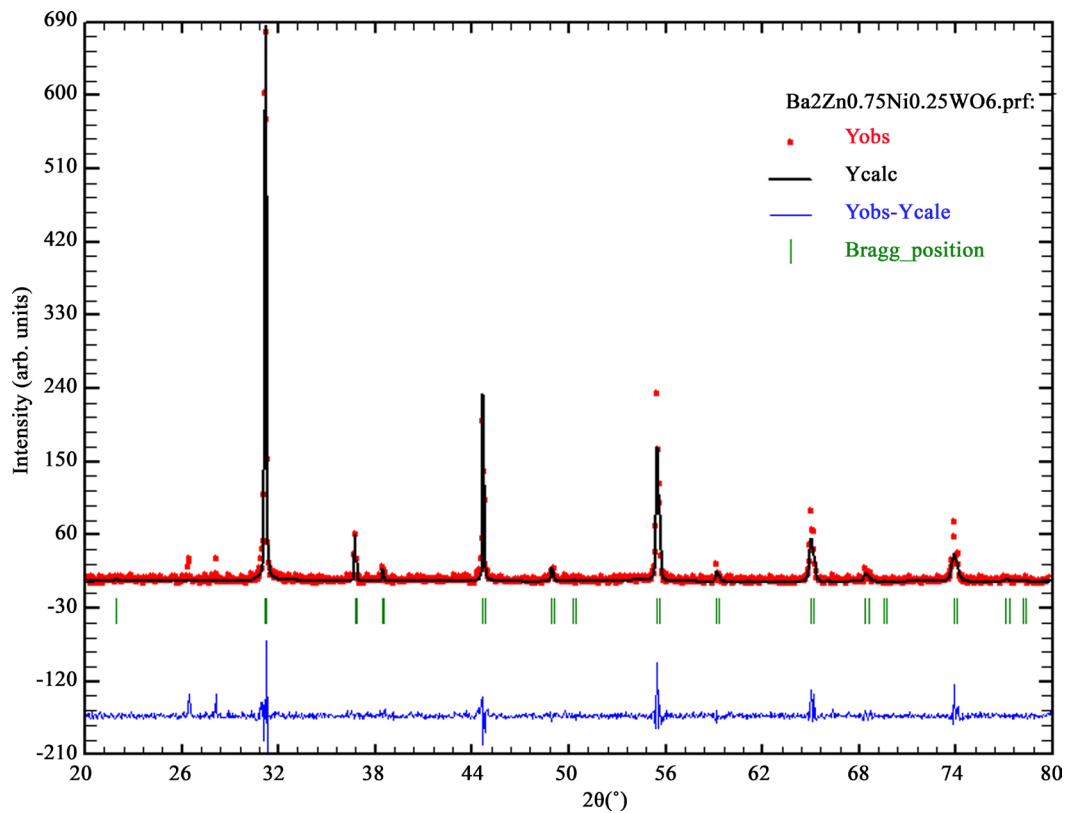
**Figure 2.** XRD pattern for selected range of  $2\theta$ .

**Table 1.** The atom positions, the space groups, the lattice parameter and crystallite size of the  $\text{Ba}_2\text{Zn}_{1-x}\text{Ni}_x\text{WO}_6$  double perovskite series where ( $x = 0, 0.25, 0.50, 0.75, 1$ ).

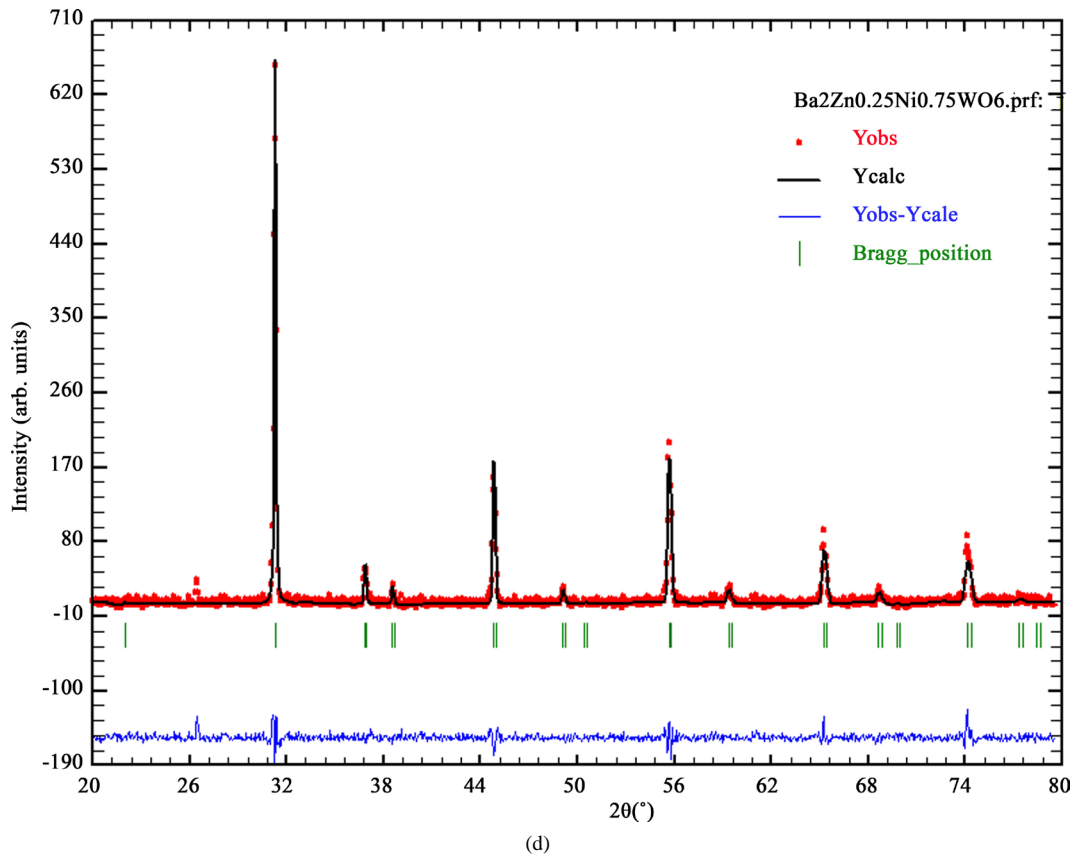
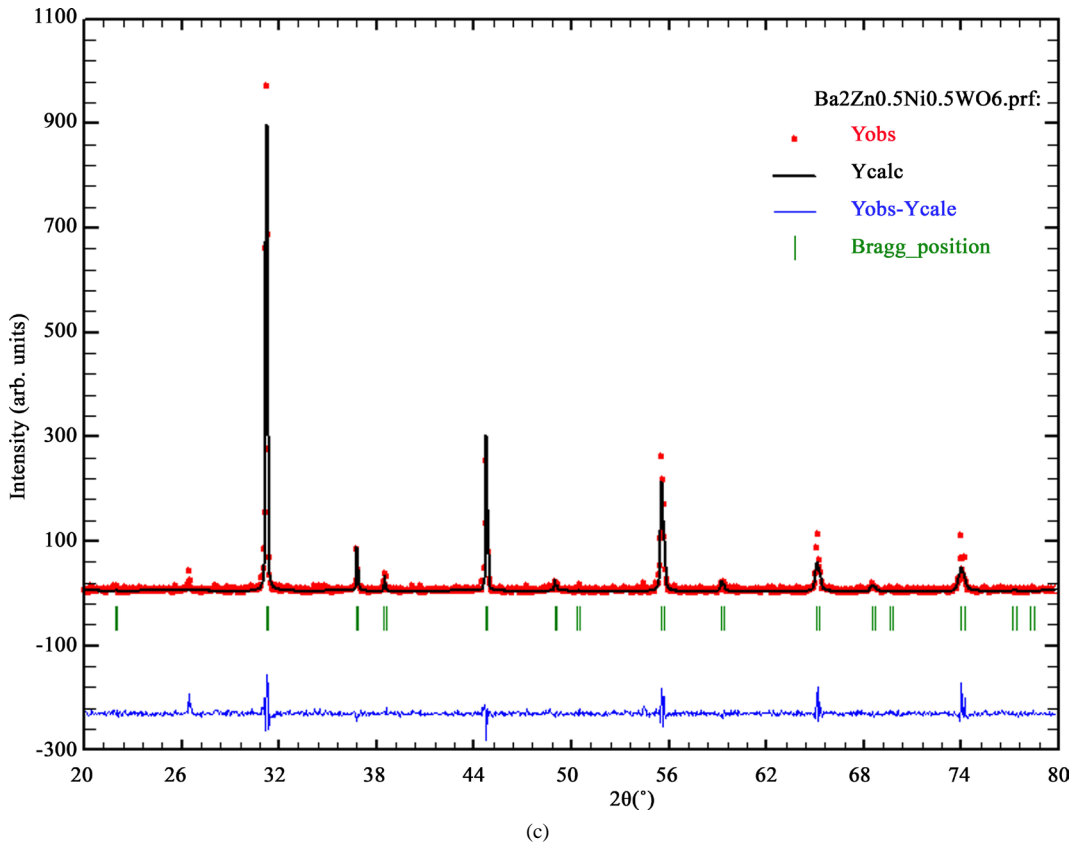
Element	Coordinates	$\text{Ba}_2\text{ZnWO}_6$	$\text{Ba}_2\text{Zn}_{0.75}\text{Ni}_{0.25}\text{WO}_6$	$\text{Ba}_2\text{Zn}_{0.50}\text{Ni}_{0.50}\text{WO}_6$	$\text{Ba}_2\text{Zn}_{0.25}\text{Ni}_{0.75}\text{WO}_6$	$\text{Ba}_2\text{NiWO}_6$
		Fm-3m	Fm-3m	Fm-3m	Fm-3m	Fm-3m
$\text{Ba}_1^{+2}/\text{Ba}_2^{+2}$	X	0.2500	0.2500	0.2500	0.2500	0.2500
	Y	0.2500	0.2500	0.2500	0.2500	0.2500
	Z	0.2500	0.2500	0.2500	0.2500	0.2500
$\text{Zn}^{+2}$	X	0.5000	0.5000	0.5000	0.5000	
	Y	0.5000	0.5000	0.5000	0.5000	
	Z	0.5000	0.5000	0.5000	0.5000	
$\text{Ni}^{+2}$	X		0.5000	0.5000	0.5000	0.5000
	Y		0.5000	0.5000	0.5000	0.5000
	Z		0.5000	0.5000	0.5000	0.5000
$\text{W}^{+6}$	X	0.0000	0.0000	0.0000	0.0000	0.0000
	Y	0.0000	0.0000	0.0000	0.0000	0.0000
	Z	0.0000	0.0000	0.0000	0.0000	0.0000
$\text{O}_1^{-2}/\text{O}_2^{-2}$	X	0.2399	0.23697	0.21735	0.23495	0.23317
	Y	0.0000	0.0000	0.0000	0.0000	0.0000
	Z	0.0000	0.0000	0.0000	0.0000	0.0000
a/b/c (nm)		8.118340	8.108754	8.097554	8.082387	8.080683
$\alpha/\beta/\gamma$		90	90	90	90	90
V ( $\text{nm}^3$ )		535.0590	533.166	530.960	527.982	527.648
Crystallite size (nm)		105.09	126.77	110.53	71.91	148.71
Tolerance factor		1.008	1.01	1.014	1.017	1.02



(a)



(b)



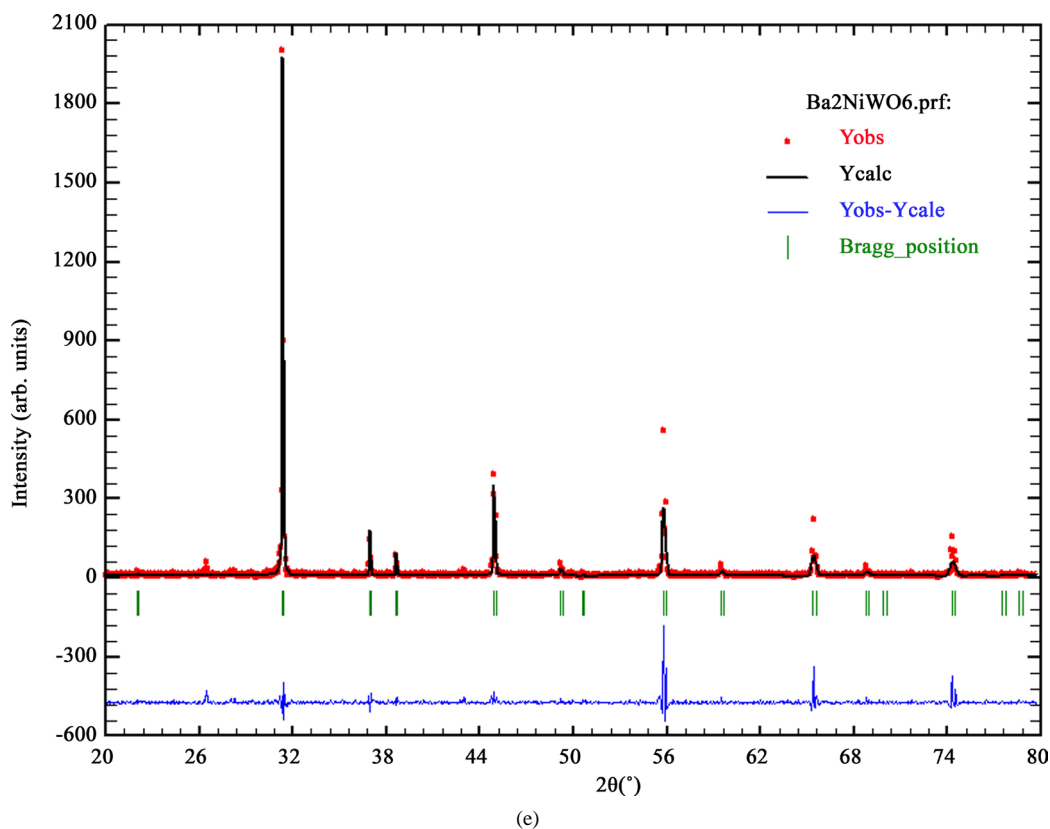


**Figure 3.** (a) Refined XRD patterns of the  $\text{Ba}_2\text{ZnWO}_6$  sample; (b) Refined XRD patterns of the  $\text{Ba}_2\text{Zn}_{0.75}\text{Ni}_{0.25}\text{WO}_6$  sample; (c) Refined XRD patterns of the  $\text{Ba}_2\text{Zn}_{0.50}\text{Ni}_{0.50}\text{WO}_6$  sample; (d) Refined XRD patterns of the  $\text{Ba}_2\text{Zn}_{0.25}\text{Ni}_{0.75}\text{WO}_6$  sample; (e) Refined XRD pattern of the  $\text{Ba}_2\text{NiWO}_6$  sample.

for the  $\text{Ba}_2\text{MWO}_6$  double perovskite samples where (M = Zn, Mg) using the Single-crystal X-ray diffraction and Neutron diffraction. Furthermore, Y. Tamraoui *et al.* [17] found the similar structure (Fm-3m) cubic structure for  $\text{Ba}_{2-x}\text{Sr}_x\text{MgTeO}_6$  series where x lies between 0 and 1.5.

From X-ray result, the cubic structure is confirmed for all samples so the Ba-cation is surrounding by 12 oxygen anions in a regular dodecahedral environment and the Zn-cation, Ni-cation, W-cation is octahedral coordinated by six oxygen ions, giving rise of  $180^\circ$  B-O-B bond angles [18] [19]. The crystallite size for  $\text{Ba}_2\text{Zn}_{1-x}\text{Ni}_x\text{WO}_6$  double perovskite series is calculated from full-width at half-maximum (FWHM) using Scherer formula for the major peaks at (220) that observed to vary between 71.91 to 148.71 nm for the samples. The tolerance factor is calculated and is found to be between (1.008 - 1.020) as shown in **Table 1**. This is confirmed the (Fm-3m) cubic structure according to the criteria adopted by Correa *et al.* and Popov *et al.* [12] [13]. **Figure 4(a)** and **Figure 4(b)** show the relation between the tolerance factor and volume of unit cell respectively with ratio of replacement. The tolerance factor of the samples is found to take almost the same value. This may be attributed to the same values of ionic radii of  $\text{Ni}^{2+}$  and  $\text{Zn}^{2+}$  cations. D. Serrate *et al.* [20] verified the rule of double perovskite tolerance factor for the (Fm-3m) cubic structure to be between 1.05 - 1.00. The volume of unit cells is found to decrease with the increasing ratio of replacement of  $\text{Zn}^{2+}$  cations by  $\text{Ni}^{2+}$  cations. This is may be due to the size of  $\text{Zn}^{2+}$  cations being larger than the size of  $\text{Ni}^{2+}$  cations.

### 3.3. The IR Spectroscopy Results

The FTIR spectra of the perovskite structure have three characteristic absorption bands between  $850 - 400\text{ cm}^{-1}$ , respective to composition and these are usually used to identify the perovskite phase formation [21]. It is based on infrared spectrum can be used for molecules such as fingerprint for humans [22]. The strong high-energy band centered at about  $620\text{ cm}^{-1}$  can be assigned to the anti-symmetric stretching mode of the (Zn- $\text{O}_6$ ), (Ni- $\text{O}_6$ ) and (W- $\text{O}_6$ ) octahedral is due to the higher charge of this cation. Another interesting point appear by this spectra

is the presence of the high intensity band at about  $825\text{ cm}^{-1}$  which can be assigned to the symmetric stretching vibration of these octahedral as explain. The positions of these bands suggests relatively long (Zn-O<sub>6</sub>), (Ni-O<sub>6</sub>) and (W-O<sub>6</sub>) bands [23] [24]. The bands appeared around  $420\text{ cm}^{-1}$  are may be due to deformational modes of the ZnO<sub>6</sub>, NiO<sub>6</sub> and WO<sub>6</sub> octahedrals. From Figure 5 that shows the transmittance of Ba<sub>2</sub>Zn<sub>1-x</sub>Ni<sub>x</sub>WO<sub>6</sub> double perovskite series versus wave number; all the samples confirmed the molecular bands on the form perovskite oxide [24]. The peak between  $1450 - 1400\text{ cm}^{-1}$  is likely corresponds to overtones of the fundamental vibrations of carbonate [25] [26].

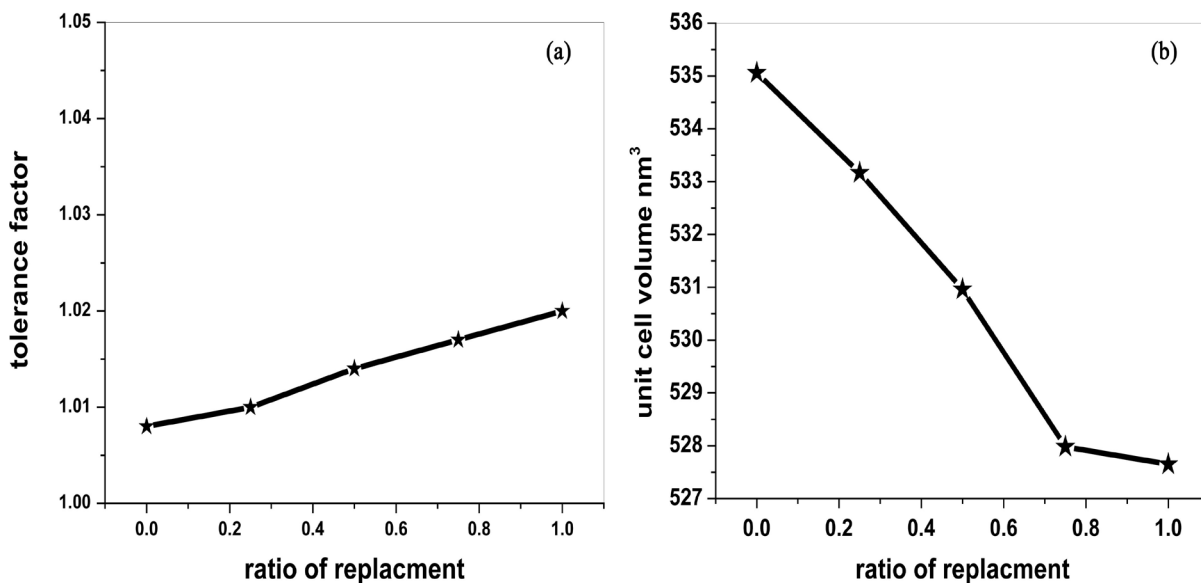


Figure 4. (a).The tolerance factor versus the ratio of replacement; (b) The volume of unit cell versus the ratio of replacement.

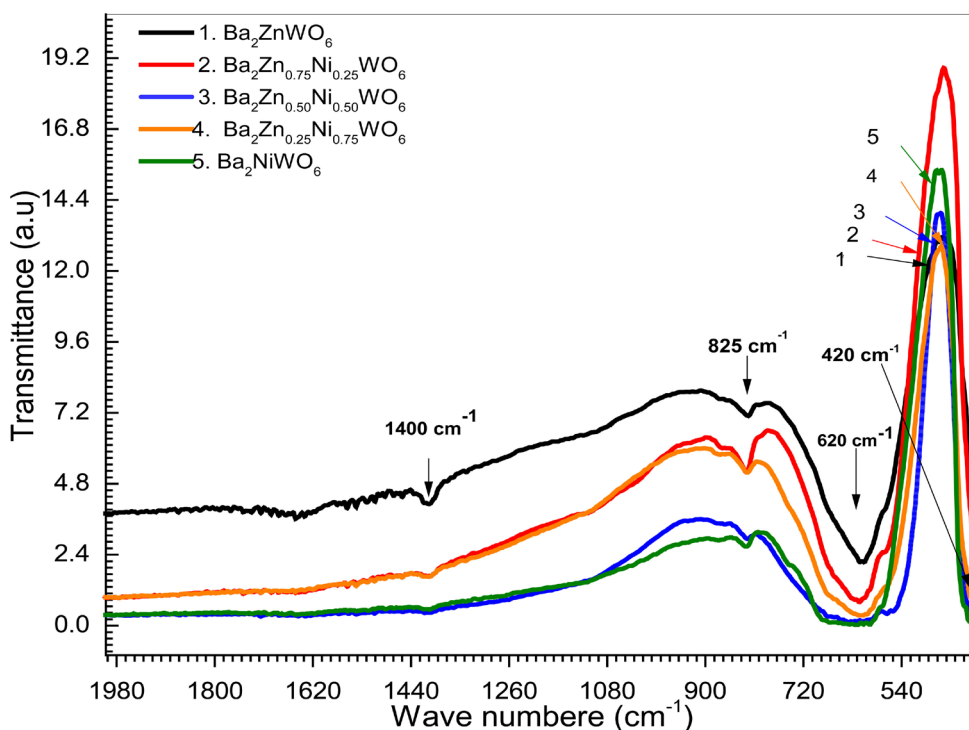


Figure 5. The IR spectra of the Ba<sub>2</sub>Zn<sub>1-x</sub>Ni<sub>x</sub>WO<sub>6</sub> double perovskite oxides.

## 4. Conclusion

The  $\text{Ba}_2\text{Zn}_{1-x}\text{Ni}_x\text{WO}_6$  double perovskite series, where  $x = 0, 0.25, 0.50, 0.75, 1$ , were synthesized using solid state method. The X-ray diffraction (XRD) and the Fourier Transform Infrared Spectroscopy (FTIR) were used as analytical tools. The XRD patterns were measured at room temperature for the series and showed the same cubic structure before and after the replacement of  $\text{Zn}^{2+}$  cation by  $\text{Ni}^{2+}$ . As a result of a convergence of the ionic radius of the  $\text{Zn}^{2+}$  cation and  $\text{Ni}^{2+}$  cation, the unit cell volume was found to decrease from  $535.059 \text{ nm}^3$  to  $527.648 \text{ nm}^3$ , while the values of tolerance factor were found to slightly increase from 1.008 to 1.02. FTIR absorption bands were found to be characteristic of perovskite structure.

## Acknowledgements

This work is supported by Materials Laboratory of Alneelain University, Khartoum, Sudan.

## References

- [1] Kim H.-S., Lee, C.-R., Im, J.-H., Lee, K.-B., Moehl, T., Marchioro, A., *et al.* (2012) Lead Iodide Perovskite Sensitized All-Solid-State Submicron Thin Film Mesoscopic Solar Cell with Efficiency Exceeding 9%. *Scientific Reports*, **2**, Article Number: 591. <http://www.nature.com/articles/srep00591#supplementary-information>.
- [2] Yang, S.H., Yan, N., Chen, S. and Zhang, Y.L. (2015) Structural and Optical Properties of the  $\text{BiFeO}_3$  System Multiferroic Films Prepared by a Sol-Gel Method. *Ceramics International*, **41**, S361-S364. <http://dx.doi.org/10.1016/j.ceramint.2015.03.210>
- [3] Peschel, S., Ziegler, B., Schwarten, M. and Babel, D. (2000) Kristallstrukturbestimmungen an  $\text{Cs}_2\text{NaCr}(\text{CN})_6$  und weiteren Verbindungen  $\text{A}_2\text{BM}(\text{CN})_6$  (A=Rb, Cs; B=Na, K, Rb,  $\text{NH}_4$ ; M=Cr, Mn, Fe, Co): Oktaederkipfung und Toleranzfaktor von Cyanokryolithen. *Zeitschrift für anorganische und allgemeine Chemie*, **626**, 1561-1566. [http://dx.doi.org/10.1002/1521-3749\(200007\)626:7<1561::AID-ZAAC1561>3.0.CO;2-J](http://dx.doi.org/10.1002/1521-3749(200007)626:7<1561::AID-ZAAC1561>3.0.CO;2-J)
- [4] Zhou, X.J., Xiao, T.J., Zhao, X.Q., Wang, Y.J., Li, L., Wang, Z.Q., *et al.* (2014) Study of the Optical Properties of Double-Perovskite  $\text{Sr}_2\text{CaW}_x\text{Mo}_{1-x}\text{O}_6$  Matrices. *Journal of Luminescence*, **152**, 165-167. <http://dx.doi.org/10.1016/j.jlumin.2013.11.045>
- [5] Tian, S.Z., Zhao, J.C., Qiao C.D., Ji, X.L. and Jiang, B.Z. (2006) Structure and Properties of the Ordered Double Perovskites  $\text{Sr}_2\text{MWO}_6$  (M = Co, Ni) by Sol-Gel Route. *Materials Letters*, **60**, 2747-2750. <http://dx.doi.org/10.1016/j.matlet.2006.01.083>
- [6] Manoun, B., Igartua, J.M., Lazor, P. and Ezzahi, A. (2012) High Temperature Induced Phase Transitions in  $\text{Sr}_2\text{ZnWO}_6$  and  $\text{Sr}_2\text{CoWO}_6$  Double Perovskite Oxides: Raman Spectroscopy as a Tool. *Journal of Molecular Structure*, **1029**, 81-85. <http://dx.doi.org/10.1016/j.molstruc.2012.05.077>
- [7] Zheng, J.D., Lang, X.F. and Wang, C.J. (2014) Effect of Preparation Method on Catalytic Properties of Double Perovskite Oxides  $\text{LaSrFeMo}_{0.9}\text{Co}_{0.1}\text{O}_6$  for Methane Combustion. *Advances in Chemical Engineering and Science*, **4**, 367-373. <http://dx.doi.org/10.4236/aces.2014.43040>
- [8] López, C.A., Curiale, J., Viola, Md.C., Pedregosa, J.C. and Sánchez, R.D. (2007) Magnetic Behavior of  $\text{Ca}_2\text{NiWO}_6$  Double Perovskite. *Physica B: Condensed Matter*, **398**, 256-258. <http://dx.doi.org/10.1016/j.physb.2007.04.073>
- [9] Bugaris, D.E., Hodges, J.P., Huq, A. and zur Loye, H.-C. (2011) Crystal Growth, Structures, and Optical Properties of the Cubic Double Perovskites  $\text{Ba}_2\text{MgWO}_6$  and  $\text{Ba}_2\text{ZnWO}_6$ . *Journal of Solid State Chemistry*, **184**, 2293-2298. <http://dx.doi.org/10.1016/j.jssc.2011.06.015>
- [10] Suryanarayana, C. and Norton, M.G. (1998) X-Rays and Diffraction. In: Suryanarayana, C. and Norton, M.G., Eds., *X-Ray Diffraction*, Springer US, Boston, 3-19. [http://dx.doi.org/10.1007/978-1-4899-0148-4\\_1](http://dx.doi.org/10.1007/978-1-4899-0148-4_1)
- [11] Singh, D. and Mahajan, A. (2015) Effect of Size Disorder on the Structure and Magnetic Properties of  $\text{La}_{0.3}\text{R}_{0.2}\text{Sr}_{0.5}\text{Ti}_{0.5}\text{Fe}_{0.5}\text{O}_3$  (R = La, Nd, Gd, and Dy) Compounds. *Journal of Sol-Gel Science and Technology*, **76**, 171-179. <http://dx.doi.org/10.1007/s10971-015-3764-7>
- [12] Corrêa, H., Cavalcante, I., Souza, D., Santos, E., Orlando, M.D., Belich, H., *et al.* (2010) Synthesis and Structural Characterization of the  $\text{Ca}_2\text{MnReO}_6$  Double Perovskite. *Cerâmica*, **56**, 193-200. <http://dx.doi.org/10.1590/S0366-69132010000200015>
- [13] Popov, G., Greenblatt, M. and Croft, M. (2003) Large Effects of A-Site Average Cation Size on the Properties of the Double Perovskites  $\text{Ba}_{2-x}\text{Sr}_x\text{MnReO}_6$ :  $\text{Ad}^p - d^l$  system. *Physical Review B*, **67**, 024406. <http://dx.doi.org/10.1103/PhysRevB.67.024406>
- [14] Kavitha, V.T., Jose, R., Ramakrishna, S., Wariar, P.R.S. and Koshy, J. (2011) Combustion Synthesis and Characterization of  $\text{Ba}_2\text{NdSbO}_6$  Nanocrystals. *Bulletin of Materials Science*, **34**, 661-665. <http://dx.doi.org/10.1007/s12034-011-0178-1>

- [15] Elbadawi, A.A., Yassin, O. and Siddig, M.A. (2015) Effect of the Cation Size Disorder at the A-Site on the Structural Properties of SrAFeTiO<sub>6</sub> Double Perovskites (A= La, Pr or Nd). *Journal of Materials Science and Chemical Engineering*, **3**, 21-29. <http://dx.doi.org/10.4236/msce.2015.35003>
- [16] Manoun, B., Ezzahi, A., Benmokhtar, S., Ider, A., Lazor, P., Bih, L., *et al.* (2012) X-Ray Diffraction and Raman Spectroscopy Studies of Temperature and Composition Induced Phase Transitions in Ba<sub>2-x</sub>Sr<sub>x</sub>ZnWO<sub>6</sub> (0 ≤ x ≤ 2) Double Perovskite Oxides. *Journal of Alloys and Compounds*, **533**, 43-52. <http://dx.doi.org/10.1016/j.jallcom.2012.03.075>
- [17] Tamraoui, Y., Manoun, B., Mirinioui, F., Haloui, R. and Lazor, P. (2014) X-Ray Diffraction and Raman Spectroscopy Studies of Temperature and Composition Induced Phase Transitions in Ba<sub>2-x</sub>Sr<sub>x</sub>MgTeO<sub>6</sub> (0 ≤ x ≤ 2). *Journal of Alloys and Compounds*, **603**, 86-94. <http://dx.doi.org/10.1016/j.jallcom.2014.03.037>
- [18] Jeng, H.-T. and Guo, G.Y. (2003) First-Principles Investigations of Orbital Magnetic Moments and Electronic Structures of the Double Perovskites Sr<sub>2</sub>FeMoO<sub>6</sub>, Sr<sub>2</sub>FeReO<sub>6</sub> and Sr<sub>2</sub>CrWO<sub>6</sub>. *Physical Review B*, **67**, Article ID: 094438. <http://dx.doi.org/10.1103/PhysRevB.67.094438>
- [19] Bhattacharjee, S. (2012) Effect of Oxygen on the Structure and Magnetic Properties of LaMnO<sub>3</sub>.
- [20] Serrate, D., Teresa, J.M.D. and Ibarra, M.R. (2007) Double Perovskites with Ferromagnetism above Room Temperature. *Journal of Physics: Condensed Matter*, **19**, Article ID: 023201. <http://dx.doi.org/10.1002/chin.200723213>
- [21] Mostafa, M.F., Ata-Allah, S.S., Youssef, A.A.A. and Refai, H.S. (2008) Electric and AC Magnetic Investigation of the Manganites La<sub>0.7</sub>Ca<sub>0.3</sub>Mn<sub>0.96</sub>In<sub>0.04x</sub>Al<sub>(1-x)0.04</sub>O<sub>3</sub>; (0.0 ≤ x ≤ 1.0). *Journal of Magnetism and Magnetic Materials*, **320**, 344-353. <http://dx.doi.org/10.1016/j.jmmm.2007.06.022>
- [22] Millis, A.J., Shraiman, B.I. and Mueller, R. (1996) Dynamic Jahn-Teller Effect and Colossal Magnetoresistance in La<sub>1-x</sub>Sr<sub>x</sub>MnO<sub>3</sub>. *Physical Review Letters*, **77**, 175-178. <http://dx.doi.org/10.1103/PhysRevLett.77.175>
- [23] Bharti, C., Das, M.K., Sen, A., Chanda, S. and Sinha, T.P. (2014) Rietveld Refinement and Dielectric Relaxation of a New Rare Earth Based Double Perovskite Oxide: BaPrCoNbO<sub>6</sub>. *Journal of Solid State Chemistry*, **210**, 219-223. <http://dx.doi.org/10.1016/j.jssc.2013.11.024>
- [24] Bharti, C., Sen, A., Chanda, S. and Sinha, T.P. (2014) Structural, Vibrational and Electrical Properties of Ordered Double Perovskite Oxide BaLaMnSbO<sub>6</sub>. *Journal of Alloys and Compounds*, **590**, 125-130. <http://dx.doi.org/10.1016/j.jallcom.2013.12.124>
- [25] Bharti, C. and Sinha, T.P. (2010) Dielectric Properties of Rare Earth Double Perovskite Oxide Sr<sub>2</sub>CeSbO<sub>6</sub>. *Solid State Sciences*, **12**, 498-502. <http://dx.doi.org/10.1016/j.solidstatesciences.2009.12.014>
- [26] Deepa, A.S., Vidya, S., Manu, P.C., Solomon, S., John, A. and Thomas, J.K. (2011) Structural and Optical Characterization of BaSnO<sub>3</sub> Nanopowder Synthesized through a Novel Combustion Technique. *Journal of Alloys and Compounds*, **509**, 1830-1835. <http://dx.doi.org/10.1016/j.jallcom.2010.10.056>